European Conference on Computational Fluid Dynamics
ECCOMAS CFD 2006
P. Wesseling, E. Oñate, J. Périaux (Eds)
© TU Delft, The Netherlands, 2006

INVESTIGATION OF THE EFFECT OF BASE BLEED ON THRUST PERFORMANCE OF A TRUNCATED AEROSPIKE NOZZLE IN OFF-DESIGN CONDITIONS

Arash Naghib-Lahouti[1], Elhaum Tolouei[2]

[1]Aerospace Research Institute, Faculty Member
PO Box 14665-834, Tehran, Iran
e-mail: lahouti@ari.ac.ir

[2]Aerospace Research Institute, Research Engineer
e-mail: tolouei@ari.ac.ir

Keywords: Aerospike Nozzle, Truncation, Base Bleed, Thrust, Numerical Analysis

Abstract. *Plug truncation is a common measure to reduce an aerospike nozzle's weight and length, and to make it more feasible for application in a rocket propulsion system. On the other hand, aerospike nozzles with larger amounts of base truncation tend to suffer loss of thrust, especially in over-expansion conditions. To reduce this loss of thrust, a technique called base bleed is used, in which a secondary flow is injected at the base of the truncated plug. Success of the base bleed technique depends on several factors, including position, direction and amount of the injected flow, as well as the nozzle's working conditions. In this report, effects of the amount of base bleed and the nozzle's working conditions on total thrust and pressure thrust generated by the base of an aerospike nozzle is numerically analyzed. The mechanism by which base bleed affects base pressure distribution and flow pattern around the plug is also studied. Based on the results of the analyses, conclusions regarding the optimum amount of base bleed in different working conditions have been derived.*

1 INTRODUCTION

Expansion and discharge of a gas in different propulsion systems, e.g. jet engines and rockets, is always accomplished by a nozzle. Thrust of a conventional nozzle with fixed geometry, discharging in atmosphere can be expressed by the following simple relation:

$$F = \dot{m}V_e + (P_e - P_{atm})A_e \quad (1)$$

This relation indicates that for a nozzle designed to have a constant value of P_e (also known as design exhaust pressure, P_{des}), thrust is affected by change of altitude. At the design altitude, where $P_{atm} = P_{des}$, the second term of the above relation (known as pressure thrust) is zero, and the nozzle is said to be working in "optimum condition". At altitudes lower than the design altitude, where $P_{atm} > P_{des}$, pressure thrust assumes a negative value, and loss of thrust is inevitable. These conditions, which occur at altitudes ranging from ground level to the design altitude, are known as “over-expansion” conditions. Beside the inherent loss of thrust, the conventional nozzle might suffer problems including shock waves and flow separation in the divergent section, thrust oscillation, and flow asymmetry in over-expansion conditions.

Ever since jet and rocket propulsion systems have emerged, researchers have different idea, mainly to increase the thrust performance of nozzles in off-design working conditions. Among these various designs, features of the aerospike nozzle have attracted researchers since mid-1950s[1]. Many theoretical studies of the aerospike nozzle have been carried out in 1960s. Berman and Crimp’s work[2] is an example of these studies, in which issues such as analytical design methods, thrust vectoring, and integration with solid- and liquid-propellant systems have been addressed. Rao[3] has presented a more accurate method based on calculus of variations for design of the plug in 1961, and Lee and Thompson[4] have developed the first computer program for plug nozzle design based on Rao’s work in 1964. In early 1970s, thermal and strength problems of the aerospike nozzle and development of more efficient methods for fabrication of conventional nozzles led to a decline in research activities in this field.

In 1990s, NASA initiated the SSTO (Single Stage to Orbit) project, which required a propulsion system with maximum efficiency in a broad range of working altitudes. The aerospike propulsion system was selected for this purpose, and extensive research and development led to successful testing of the RS2200 aerospike engine[5]. Cancellation of this project in 2001 has led to another decline in research activities in this field in the United States in the recent years, but the aerospike nozzle is still a live research topic in Europe and Japan. Hageman et al.[6,7] have proposed application of a large scale aerospike nozzle in the post-Ariane 5 launch vehicles to DLR. Tomita et al.[8] and Sakamoto et al.[9] have carried out experimental studies of axisymmetric and linear aerospike nozzles, and Fujii and Ito[10] have studied many aspects of aerospike nozzles numerically.

Most recently, two groups in the United States have applied the axisymmetric aerospike nozzle in propulsion system of sounding rockets, and demonstrated considerable gain in the rockets’ performance[11,12].

The authors have shown in their previous work[13], that aerospike nozzles have a distinct thrust advantage over the conventional nozzle, especially in over-expansion conditions. However, practical concerns have prevented manufacturers from practically implementing this design in large-large scale propulsion systems. One of the most important concerns is the relatively large length and heavy weight of an ideal plug. Moreover, an ideal plug has a sharp end, which is susceptible to deformation at high temperatures associated with exhaust gasses of a rocket engine[14].

A common practice to overcome these problems is plug truncation (Figure 1). The authors’ previous studies of the effect of plug truncation on thrust performance of an aerospike nozzle in order to determine the appropriate amount of plug truncation, in which performance of nozzles with %100, %75, %50 and %25 plugs have been compared in different working condtions[15], have shown that:

- In under-expansion conditions, plug truncation has a negligible effect on total thrust, because the loss of thrust caused by plug truncation is compensated by the thrust generated by positive relative pressure at the base of the plug.

- In over-expansion conditions, increased plug truncation causes greater loss of thrust, because of the negative relative pressure prevailing at the base of plug, which generates negative base thrust. The gross amount of negative base thrust increases when a greater portion of the plug is truncated, and a larger base surface is exposed to negative relative pressure.

Based on these results, it can be inferred that although selecting of a plug with maximum possible base truncation would reduce the nozzle's weight and length without affecting its performance in over-expansion conditions, it would also cause the greatest loss of thrust in over-expansion conditions.

A well-known remedy for reducing loss of thrust in over-expansion conditions is base bleed, i.e. injection of a secondary flow at the base to increase overall base pressure. However, success of this remedy depends on many factors, including position, direction and amount of the injected flow, as well as the nozzle's working conditions.

Ito and Fujii[16] have studied effects of position and direction of base bleed on base thrust and flow characteristics, for one amount of base bleed (%2 of total mass flow) and one set of external flow properties (corresponding to under-expansion conditions). Their study shows that the greatest increase in base thrust can be achieved by injecting the secondary flow at a direction parallel to the nozzle's axis, and as close as possible to the perimeter of the base surface.

To complement their studies, the present work intends to investigate the effect of the two other factors affecting base bleed effectiveness. In the following chapters, effect of the amount of base bleed on base thrust and flow pattern will be analyzed, and in each case the effect of variation of ambient conditions from under-expansion to over-expansion will be studied.

To accomplish this objective, internal and external flow of a truncated aerospike nozzle with 5 values of base bleed ranging from 0% to 5% of the nozzle's total mass flow will be numerically analyzed. For each case, 6 sets of external flow conditions with ambient to design pressure ratios from 0.1 to 4.0 will be applied to cover the entire range of the nozzle's working conditions.

2 NUMERICAL MODELING AND ANALYSIS

Details of numerical modeling and analysis of internal external flow of aerospike nozzles have been extensively described in[13],[15]. However, some aspects of numerical modeling which are specifically important in analysis of aerospike nozzles with base bleed are highlighted herein:

2.1 Geometry

The baseline geometry is an aerospike nozzle with a 25% length (75% truncated) plug, whose details appear in[15]. The nozzle's plug length is 0.03143m, and the plug's base radius is 0.02091m.

Considering the results presented in[14], in order to obtain maximum bleed effectiveness, the secondary flow is injected through a circular slot at the circumference of the base surface, where distance from the nozzle's axis is maximum (Fig.2). Area of the slot is assumed to be 2% of the nozzle's inlet area:

$A_{bleed}=0.02A_{inlet}=1.4428*10^{-4}m^2$
$r_{bleed}=0.01978m$

2.2 Grid and boundary conditions

In order to facilitate definition of different initial conditions in different areas of the solution domain, which is essential in obtaining a converged solution, the solution domain is divided into 4 regions named Fluid1-Fluid4, as explained in[13] and shown in fig.3. Grid and boundary conditions in Fluid1, Fluid3, and Fluid4 regions, which contain the convergent section of the nozzle and the surrounding atmosphere are similar to those explained in[13]. In the Fluid2 region, which contains the plug, a segment of the solid wall representing the base surface which lies between r_{bleed} and r_{base}, is replaced by a mass flow inlet boundary (fig4).

The fluid2 region is discretized again using an unstructured grid of 20157 triangular cells, whose density increases near the base surface. Total number of cells in the solution domain is 96453.

2.3 Fluid properties and analysis features

Average properties of combustion products resulting from chemical reaction of ethanol and oxygen have been assumed for the fluids in all regions. These properties, which satisfy the following relation:

$$C_P = \frac{\gamma \Re}{\mathcal{M}(\gamma - 1)} \tag{2}$$

are as follows:

$\gamma = 1.21$, $C_P = 1286.68$ J/kgK, $\mathcal{M} = 37.23$ g/mol.

Combustion products have been assumed to behave as a viscous (laminar) and compressible ideal gas ($P=\rho RT$). The coupled implicit method described in[17] has been used for solution of the four governing equations (continuity, conservation of momentum in longitudinal and radial directions, and conservation of energy), considering severe compressibility effects existing in the solution domain. Fluxes of convected variables at cell walls are approximated by the first order upwind scheme. Courant's number has been set to 0.9 for all cases. Two criteria have been posed for convergence. One is reduction of the global residual of solution of all governing equations to the order of 10^{-5}, and the other is establishment of mass balance among inlet, far-field and outlet boundaries, which is checked by integration of mass flow through the mentioned boundaries in each iteration. In all cases, the solution process has been continued until both criteria are satisfied.

2.4 Analysis cases

To investigathe the effect of the amount of the injected flow, 5 cases with base bleed flow rates from 0 to 5% the nozzle's total mass flow have been analyzed. Base bleed mass flow rates for these cases appear in table 1.

Case No.	Percentage of tatal mass flow	Injected mass flow (kg/s)
1	0.0%	0
2	1.0%	0.0325758
3	2.0%	0.0651516
4	3.5%	0.1140153
5	5.0%	0.1628790

Table 1 : Base bleed mass flow rates

For each value of base bleed flow rate, nozzle's internal and external flow has been analyzed in 6 ratios of ambient to design pressure (P_{atm}/P_{des}) ranging from 0.1 to 4.0, which correspond to under-expansion, optimum, and over-expansion conditions. External flow conditions in these cases appear in table 2.

Case No.	P_{atm}/P_{des}	$P(N/m^2)$	M
1	4.00	257736	1.5
2	3.10	200000	1.5
3	1.57	101325	1.5
4	1.00	64436	2.80434
5	0.41	26415	2.5
6	0.10	6410	3.0

Table 2 : Far-field boundary values for different analysis cases

Numerical analysis has been carried out in all combinations of the cases specified in tables 1 and 2 (a total of 30 cases). In all case, pressure and temperature of the injected flow have been assumed to be equal to the nozzle's design exit values (case 4 of table 2), while velocity of injected flow differs for each case, and is proportional to base bleed mass flow rate.

3 RESULTS AND DISCUSSION

Effect of the amount of base bleed on the nozzle's thrust, base pressure distribution and base flow pattern is studied in this section, in order to understand the mechanism by which base bleed affects the mentioned parameters, and to determine the appropriate amount of base bleed flow rate considering the nozzle's working conditions.

3.1 Total base thrust

Thrust of a truncated aerospike nozzle with base bleed comprises of the following components:

1- Momentum thrust of the convergent section
2- Pressure thrust of the convergent section
3- Thrust resulting from pressure distribution on the plug's circumferential surface
4- Thrust resulting from pressure distribution on the solid portion of the base surface
5- Momentum thrust resulting from secondary flow injection
6- Pressure thrust resulting from secondary flow injection

Since flow from the throat to the end of the plug's circumferential surface is entirely supersonic, pressure waves resulting from flow phenomena at base can not move upstream. Therefore, flow around the plug remains unaffected and the first three components of the nozzle’s thrust can be assumed to be independent of base bleed. This assumption can be verified by checking values of the first three components in the numerical results.

On the other hand, total base thrust, which is the sum of the last three components, is variable and depends on the amount of base bleed. The following relation, which was originally introduced in[13], is used to obtain non-dimensional values of total base thrust:

$$C_{F_{base}} = \frac{F_{base}}{\frac{1}{2}\gamma P_{des} M_e^2 S_{base}} \qquad (3)$$

Figure 5 displays variation of non-dimensional total base thrust (C_{Fbase}) with pressure ratio (P_{atm}/P_{des}) for different amounts of base bleed.

It can be observed that base bleed increases total base thrust at all pressure ratios, and for each pressure ratio this increase in total base thrust is proportional to the amount of base bleed. The figure also shows that total base thrust decreases when ambient pressure is increased. When no base bleed is applied, total base thrust can even assume negative values in pressure ratios higher than 1. It can be seen that this trend can be slowed down or even reversed with application of base bleed.

If total base thrust is considered as the performance criterion for base bleed, one can infer from the above-mentioned results that the best amount of base bleed is the highest achievable amount. But before reaching a final conclusion, one should note that momentum thrust resulting from injection of the secondary flow is a prevailing component of total base thrust. The origin of the secondary flow in a rocket propulsion system is same as the main exhaust flow, which can be the combustion chamber in case of a solid-propellant system, or the gas generator in case of a liquid-propellant system. One way or the other, in a non-airbreathing propulsion system, tapping the main flow for injection of a secondary flow at the base would cause a loss of mass and momentum flow rate in the main flow. Even if one assumes that tapping the combustion chamber or gas generator would not reduce pressure of the main flow, the associated loss of momentum and mass flow rate would cause a reduction in the momentum thrust which could be derived from the main flow. This loss of main flow momentum thrust would in turn cancel the momentum thrust gained from secondary flow injection (the 5^{th} component of total base thrust).

It can be concluded that total base thrust is not a suitable criterion for studying effectiveness of base bleed, and that the momentum thrust resulting from secondary flow injection should not be included in such a criterion.

3.2 Base pressure thrust and average base pressure

Base pressure thrust is sum of the thrust resulting from pressure distribution one the solid surface of the base, and the pressure thrust resulting from secondary flow injection. Figure 6 displays variation of non-dimensional base pressure thrust with pressure ratio (P_{atm}/P_{des}) for different amounts of base bleed. It can be observed that in under-expansion conditions, the highest base pressure thrust is achieved with 2% base bleed, and that larger and smaller amounts of base bleed generate values of base pressure thrust less than the one achieved with 2% base bleed.

This trend continues for pressure ratios up to 1.57, where non-dimensional base pressure thrust becomes almost equal for all amounts of base bleed. For higher pressure ratios, which correspond to over-expansion conditions, the trend is reversed, and increase in base bleed causes base pressure thrust to increase.

Figure 7 displays variation of average base pressure with pressure ratio (P_{atm}/P_{des}) for different amounts of base bleed. Average base pressure, which is closely related to base pressure thrust, and is calculated using the following relation:

$$P_{avg.} = \frac{\int_{S_{base}} PdA}{S_{base}} \tag{4}$$

remains independent of ambient pressure in under-expansion conditions. This constant value is maximum for 2% base bleed.

In over-expansion conditions, average base pressure rises as ambient pressure increases, and its rate of increase is higher for larger amounts of base bleed.

Results presented in this section are in agreement in those presented in[16], where stated 2% base bleed is selected for analysis of the nozzle's performance in under-expansion conditions. This has encouraged the authors to further investigate the mechanism by which base bleed affects base pressure distribution and flow pattern.

3.3 Base pressure distribution and flow pattern

Figure 8 shows pathlines around the base of the plug in under-expansion conditions (P_{atm}/P_{des} =0.1) for different amounts of base bleed. It can be seen that the dominant flow phenomenon around the base is a pair of symmetrical vortices, which cause two stagnation points to form. One stagnation point is at the center of the base surface, and the other is further downstream on the nozzle's axis. A series of compression waves originating from the base circumference can also be noticed, which are formed at the intersection of the nozzle's exhaust flow and the injected flow.

It can be observed that while lower amounts of base bleed (1% and 2%) tend to weaken the vortices without causing them to move, for higher amounts of base bleed (3.5% and 5%), strong circumferential compression waves cause the base vortices to grow stronger and move towards the base surface.

Effect of this change of base vortex position and strength can be seen in figure 10, which displays base pressure distribution at P_{atm}/P_{des} =0.1 for different amount of base bleed. The figure shows that the highest values of base pressure at intermediate and circumferential areas of the base surface, which have the greatest role in producing base pressure thrust, are obtained with 2% base bleed. Higher amounts of base bleed cause a decrease of pressure in these areas and an increase of pressure in the central area of the base, leading to lower overall values of base pressure thrust.

Figure 9 shows pathlines around the base of the plug in over-expansion condition (P_{atm}/P_{des} =4.0) for different amounts of base bleed. It can be observed that in this case, the circumferential compression waves grow stronger as base bleed is increased, and cause pressure in the areas near the base surface to increase. But contrary to under-expansion conditions, they do not cause base vortices to move, even at high amounts of base bleed. The result is an increase of pressure in circumferential and intermediate areas of the base surface, with highest values obtained with 5% base bleed (figure11).

4 CONCLUSION

Results of numerical modeling of internal and external flow of a truncated aerospike nozzle with different amounts base bleed in under-expansion, optimum and over-expansion working conditions, which have been analyzed to obtain the nozzle's base thrust, base pressure distribution and flow pattern, indicate that:

1- In all working conditions, total base thrust increases as the amount of base bleed is increased. But total base thrust is not an appropriate criterion for effectiveness of base bleed, because it overlooks the loss of the nozzle's mainstream momentum thrust because of tapping the main flow for base bleed.

2- The maximum value of base pressure thrust, which does not include the momentum thrust resulting from secondary flow injection, and therefore does not have the shortcoming of the above-mentioned criterion, is obtained with 2% base bleed in under-expansion conditions, and with 5% base bleed in over-expansion conditions. Average base pressure follows the same trend, while it remains independent of ambient pressure in under-expansion conditions.

3- The dominant phenomena in flow around the base of truncated plug with base bleed are a pair of symmetrical vortices, and a series of compression waves originating from circumference of the base surface. Interaction of these phenomena affects pressure distribution on the base surface. Maximum pressure at intermediate and circumferential areas of the base surface is obtained with 2% base bleed in under-expansion conditions, and with 5% base bleed in over-expansion conditions.

In general, it can be concluded that while base bleed improves base thrust and therefore total thrust of a truncated aerospike nozzle, the flying vehicle's working conditions must be considered when selecting the appropriate amount of base bleed. For a propulsion system whose major part of flight profile is at altitudes higher than design altitude (e.g. vacuum or less dense layers of atmosphere), a moderate amount of base bleed around 2% is the best choice. Alternatively, to obtain the best performance from a propulsion system which is expected to spend most of its burn time at altitudes lower than design altitude, or in thick atmosphere, the maximum achievable amount of base bleed should be considered.

REFERENCES

[1] D. P. Hearth and G. C. Gorton, "Investigation of Thrust and Drag Characteristics of a Plug-Type Exhaust Nozzle", *NACA RM E53L16* (1954).

[2] K. Berman and F. W. Crimp Jr., "Performance of Plug-Type Rocket Exhaust Nozzle", *ARS Journal*, Jan. (1961).

[3] G.V.R. Rao, "Spike Nozzle Contour for Optimum Thrust", *Ballistic Missile and Space Technology, Vol. 2*, C. W. Morrow (Ed.), Pergamon Press, New York, pp. 92-101, (1961).

[4] C. Lee, and Thompson D., "FORTRAN Program for Plug Nozzle Design", *NASA TM X-53019*, (1964).

[5] J. Korte, J. Dunn, A. Salas, N. Alexandrov, W. Follett, G. Orient and A. Hadid, "Multidisciplinary Approach to Linear Aerospike Nozzle Optimization", *33rd Joint Propulsion Conference*, Seattle, USA, July (1997).

[6] G. Hagemann, H. Immich, T. V. Nguyen and D.E. Dumnov, "Advanced Rocket Nozzles", *Journal of Propulsion and Power*, Vol 14, No 5, pp. 620-634, AIAA, (1998).

[7] G. Hagemann, A. Preuss and H. Immich, "Advanced Nozzle Concepts for Future Rocket Engine Applications", *CNES-AAAF-ESA Conference*, Liege, Belgium, Dec.(2002).

[8] T. Tomita, Tamura H. and Takahashi M., "An Experimental Evaluation of Plug Nozzle Flow Fields", *AIAA Paper 96-2632*, (1996).

[9] H. Sakamoto, Takahashi M., Sasaki, M., Tomita, T., Kusaka K. and Tamura H., "An Experimental Study on a 14KN Linear Aerospike Nozzle Combustor", *AIAA Paper 99-2761*, (1999).

[10] T. Ito, K. Fujii and A.Koich-Hayashi, "Computations of the Axisymmetric Plug Nozzle Flow Fields", *17th AIAA Applied Aerodynamics Conference*, Norfolk, USA, June (1999).

[11] E. Besnard, H. H. Chen, T. Mueller and J. Garvey, "Design, Manufacturing and Test of a Plug Nozzle Rocket Engine", *AIAA Paper 2002-4038*, (2002).

[12] Anon., "New Nozzle Shows Potential for Increased Efficiency", *Aviation Week and Space Technology*, March 31, (2003).

[13] A. Naghib-Lahouti, M. Nazarinia, and E. Tolouei, , "Design and CFD Analysis of an Aerospike Nozzle to Compare Its Off-Design Performance with a Conventional Nozzle", *Proceedings of IMEC2004, International Mechanical Engineering Conference*, IMEC2004-FM014-CP, December 5-8, Kuwait, (2004).

[14] EAC: Environmental Aeroscience Corporation, Aerospike Development Program, 2005, Available [on-line]: http://www.hybrids.com/aerospike.htm

[15] M. Nazarinia, A. Naghib-Lahouti and E. Tolouei, “Design and numerical analysis of aerospike nozzles with different plug shapes to compare their performance with a conventional nozzle”, *The Eleventh Australian International Aerospace Congress, Melbourne, Australia*, 13-17 March (2005).
[16] T. Ito, K. Fujii, “Numerical Analysis of the Base Bleed Effect on the Aerospike Nozzles”, *40th AIAA Aerospace Sciences Meeting and Exhibit, Reno, Nevada, USA,* Jan. (2002).
[17] Anon. *,FLUENT 5.23 User’s Guide*, FLUENT Inc., Lebanon, NH, USA, (1999).

FIGURES

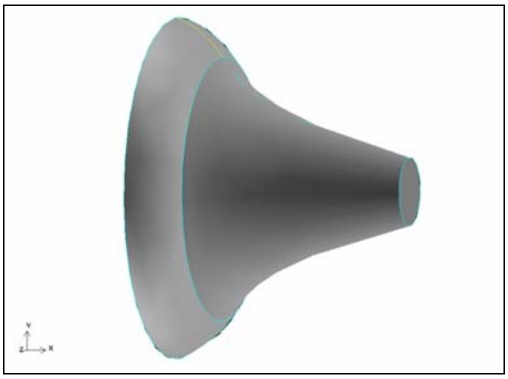

Figure 1: Truncated plug

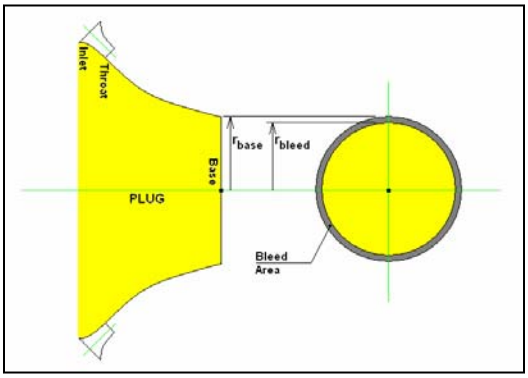

Figure 2: Geometry of truncated plug with base bleed

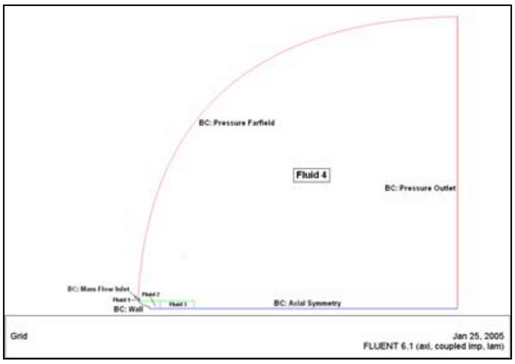

Figure 3: Numerical solution domain and boundary conditions

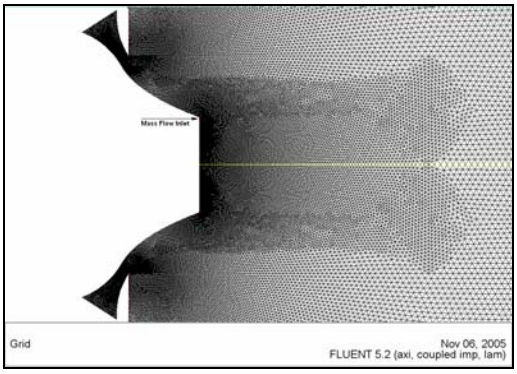

Figure 4: Close up of the unstructured grid around the plug

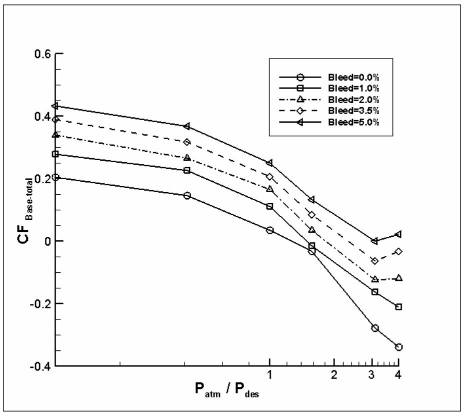

Figure 5: Total base thrust plotted against ambient pressure for different amounts of base bleed

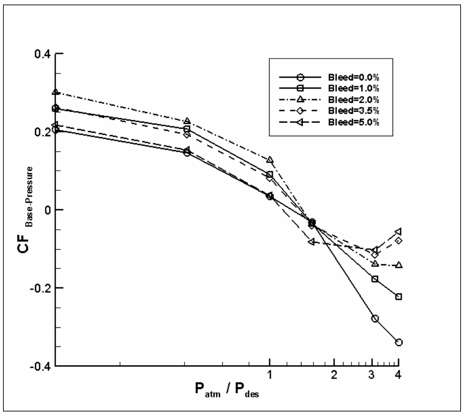

Figure 6: Base pressure thrust plotted against ambient pressure for different amounts of base bleed

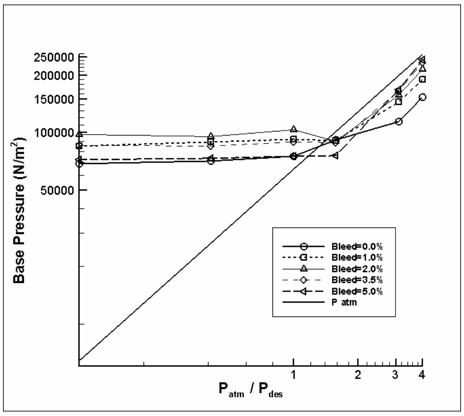

Figure 7: Average base pressure plotted against ambient pressure for different amounts of base bleed

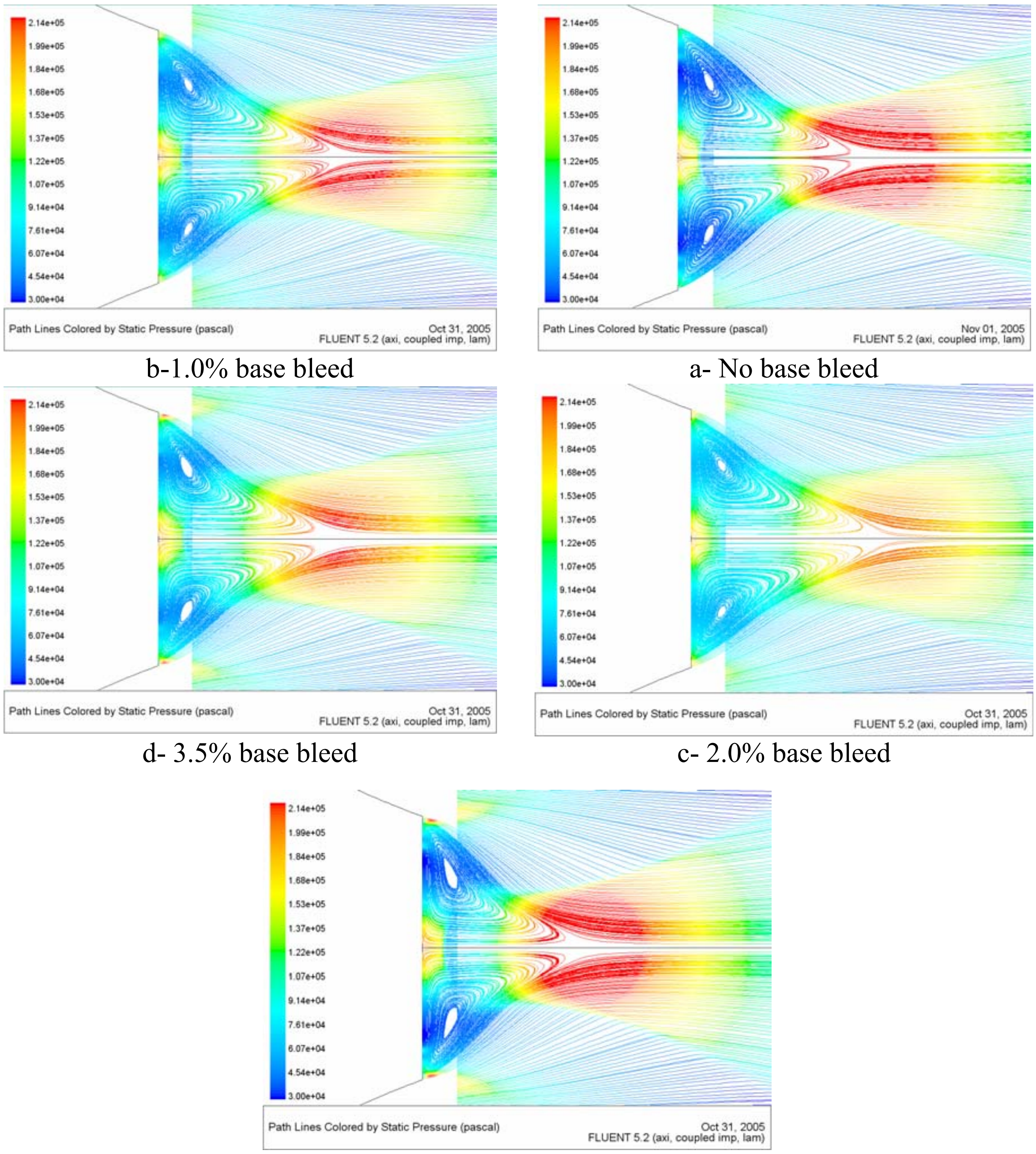

Figure 8: Pathlines colored by static pressure for different amounts of base bleed at $P_{atm}/P_{des} = 0.1$

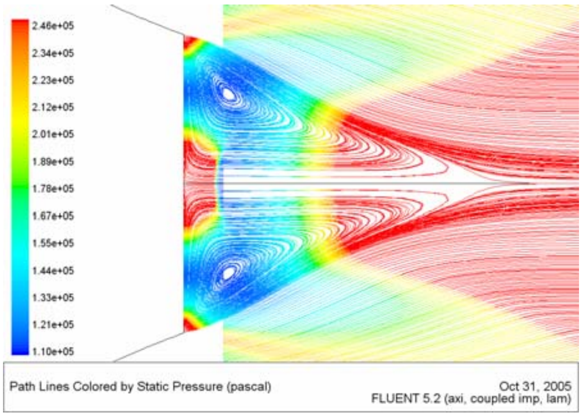

b- 1.0% base bleed

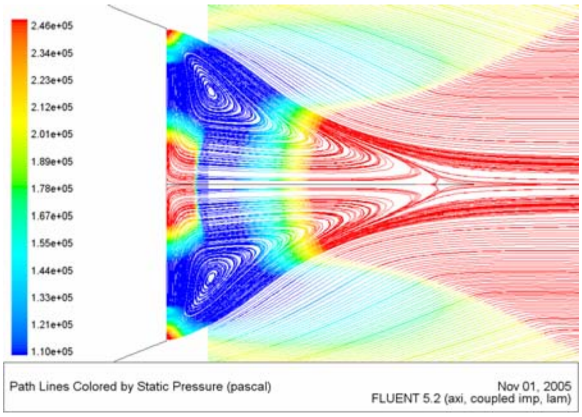

a- Zero base bleed

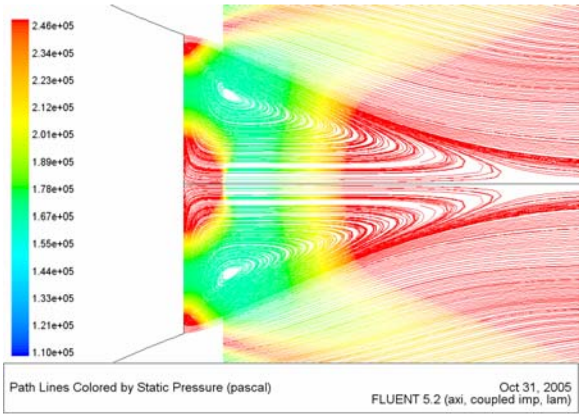

d- 3.5% base bleed

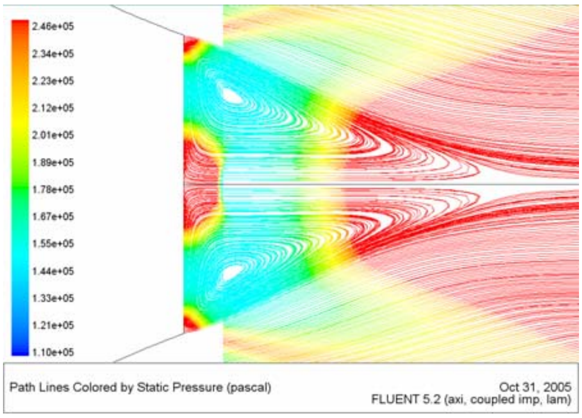

c- 2.0% base bleed

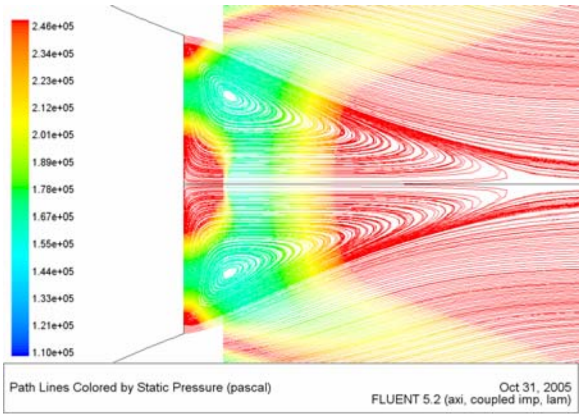

e- 5.0% base bleed

Figure 9: Pathlines colored by static pressure for different amounts of base bleed at $P_{atm}/P_{des}=4.0$

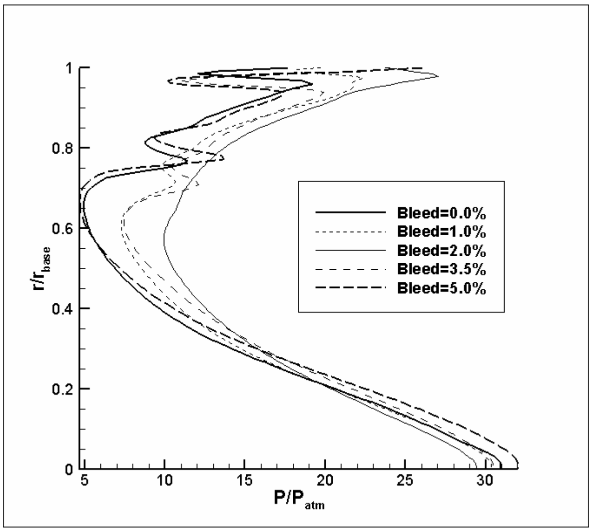

Figure 10: Base pressure distribution for different amounts of base bleed at P_{atm}/P_{des} =0.1

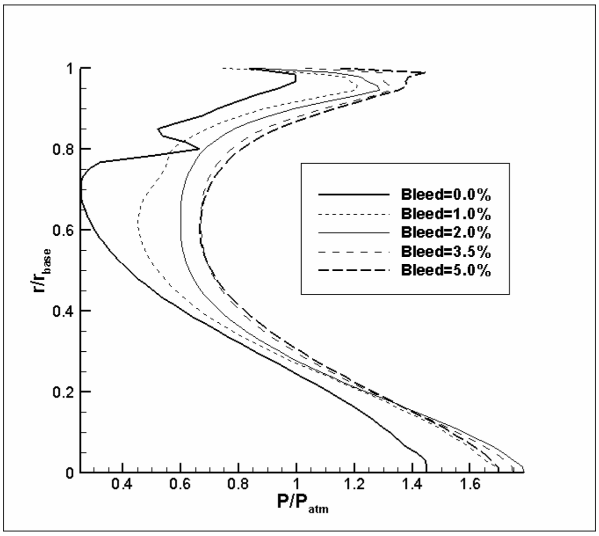

Figure 11: Base pressure distribution for different amounts of base bleed at P_{atm}/P_{des} =4.0